

Low-energy ^{23}Al β -delayed proton decay and ^{22}Na destruction in novae

M. Friedman^{1,2,*} T. Budner^{1,3} D. Pérez-Loureiro^{1,4} E. Pollacco⁵ C. Wrede^{1,3,†} J. José^{6,7} B. A. Brown^{1,3} M. Cortesi¹ C. Fry^{1,3} B. Glassman^{1,3} J. Heideman⁴ M. Janasik^{1,3} M. Roosa^{1,3} J. Stomps^{1,3} J. Surbrook^{1,3} and P. Tiwari^{1,3}

¹National Superconducting Cyclotron Laboratory, Michigan State University, East Lansing, Michigan 48824, USA

²Racah Institute of Physics, Hebrew University, Jerusalem, Israel 91904

³Department of Physics and Astronomy, Michigan State University, East Lansing, Michigan 48824, USA

⁴Department of Physics and Astronomy, University of Tennessee, Knoxville, Tennessee 37996, USA

⁵IRFU, CEA, Université Paris-Saclay, F-91191, Gif-sur-Yvette, France

⁶Departament de Física, Escola d'Enginyeria de Barcelona Est, Universitat Politècnica de Catalunya, Avenida/Eduard Maristany 10, E-08930 Barcelona, Spain

⁷Institut d'Estudis Espacials de Catalunya, Edifici Nexus-201, C/Gran Capità 2-4, E-08034 Barcelona, Spain



(Received 21 November 2019; revised manuscript received 12 February 2020; accepted 23 March 2020; published 19 May 2020)

The radionuclide ^{22}Na is a target of γ -ray astronomy searches, predicted to be produced during thermonuclear runaways driving classical novae. The $^{22}\text{Na}(p, \gamma)^{23}\text{Mg}$ reaction is the main destruction channel of ^{22}Na during a nova, hence, its rate is needed to accurately predict the ^{22}Na yield. However, experimental determinations of the resonance strengths have led to inconsistent results. In this Rapid Communication, we report a measurement of the branching ratios of the ^{23}Al β -delayed protons as a probe of the key 204-keV (center-of-mass) $^{22}\text{Na}(p, \gamma)^{23}\text{Mg}$ resonance strength. We report a factor of 5 lower branching ratio compared to the most recent literature value. The variation in ^{22}Na yield due to nuclear data inconsistencies was assessed using a series of hydrodynamic nova outburst simulations and has increased to a factor of 3.8, corresponding to a factor of ≈ 2 uncertainty in the maximum detectability distance. This is the first reported scientific measurement using the Gaseous Detector with Germanium Tagging system.

DOI: [10.1103/PhysRevC.101.052802](https://doi.org/10.1103/PhysRevC.101.052802)

Radionuclides are now routinely observed astronomically using space-based γ -ray observatories capable of detecting their characteristic emission lines. For example, ^{26}Al ($T_{1/2} = 0.72$ Ma) and ^{60}Fe ($T_{1/2} = 2.6$ Ma) live long enough to migrate from the stellar events producing them before they decay and manifest as diffuse emission across the Milky Way. Attempts have been made to benchmark nucleosynthesis in massive stars and their supernovae using the relative amounts of observed ^{26}Al [1–5] and ^{60}Fe [6], but such benchmarks can only be applied by considering all possible sources in aggregate. More stringent constraints on astrophysical models of particular events can be derived using shorter-lived nuclides that manifest as localized sources, such as ^{44}Ti ($T_{1/2} = 59$ a), which has been observed in the 350-yr-old Cas A core-collapse supernova remnant [7–11] and the younger remnant of Supernova 1987A [12]. Similarly, the detection of ^{22}Na ($T_{1/2} = 2.6$ a) from a classical nova explosion has been a long sought constraint [13–19]. Observations with previously and currently deployed instruments may have been on the cusp of detecting ^{22}Na [20–25], and more sensitive future missions are being planned [26,27]. Accurate model predictions of ^{22}Na nucleosynthesis in novae are needed to estimate the

detectability distance and for comparison to past searches and future observations. In addition, $^{20}\text{Ne}/^{22}\text{Ne}$ ratios in presolar grains may be used to identify presolar nova grains [28–31]. Usually, neon is incorporated in grains via implantation since noble gases do not condense as stable compounds into grains. However, low $^{20}\text{Ne}/^{22}\text{Ne}$ ratios suggest that ^{22}Ne originated from *in situ* decay of ^{22}Na .

The ^{22}Na yield predicted by nova models is sensitive to the thermonuclear rates of the reactions associated with explosive hydrogen burning on the surface of a white-dwarf star accreting hydrogen-rich material from a binary companion star [19,32]. This has motivated the development of innovative experimental nuclear physics techniques, providing rates to improve predictions of the ^{22}Na yield [33–45]. While ^{22}Na is being produced during the thermonuclear runaway driving a nova, the $^{22}\text{Na}(p, \gamma)^{23}\text{Mg}$ reaction is actively destroying it. The ^{22}Na yield is related inversely to the reaction rate and, in particular, to the strength of a single resonance at a center-of-mass energy of 204 keV.¹ Two direct measurements ([34,35] and [43,44]) of the resonance strength using proton beams and radioactive ^{22}Na targets have yielded values that differ by a factor of 3.2, which results in a factor of ≈ 2 variation

*moshe.friedman@mail.huji.ac.il

†wrede@nscl.msu.edu

¹This resonance is referred to by the 213-keV proton laboratory energy in some publications [35,44].

in the expected ^{22}Na yield from classical novae [43]. Another way to determine the strength is to combine measurements of the proton branching ratio Γ_p/Γ of the resonance with its lifetime τ and spin. The most precise literature values [41,45] for these quantities yield a strength that is consistent with that from Refs. [34,35]. It may be tempting to consider this the conclusive arbiter for the two inconsistent directly measured values, but it would be prudent to confirm the proton branching ratio and lifetime as the aforementioned experiments faced significant challenges.

In particular, the $^{23}\text{Al}(\beta p)$ experiment of Ref. [45] suffered from overwhelming β background and relied heavily on a background subtraction model. Pollacco *et al.* [46] showed that a gas-filled detector can be used to overcome this problem and found indications of a branching ratio for the 204-keV level significantly lower than in Ref. [45]. Presently, we report a new proton branching ratio for the 204-keV resonance, determined based on measurements of low-energy ^{23}Al β -delayed protons with a new system: the Gaseous Detector with Germanium Tagging (GADGET) [47]. GADGET is optimized for the detection of low-energy low-intensity β -delayed protons with complementary high-resolution high-efficiency γ -ray detection. This Rapid Communication reports the first scientific results from GADGET.

The experiment was performed at the National Superconducting Cyclotron Laboratory (NSCL) where a radioactive beam of ^{23}Al was produced by projectile fragmentation. A 150-MeV/u, 75-pnA primary beam of ^{36}Ar was accelerated using the Coupled Cyclotron Facility [48] and impinged upon a ^9Be transmission target, 1363 mg/cm² in thickness. ^{23}Al was isolated in flight to a purity of 69% using the A1900 magnetic fragment separator [49] incorporating a 300-mg/cm² Al wedge and the Radio Frequency Fragment Separator (RFFS) [50]. Upon exiting the RFFS, situated about 6 m upstream of GADGET, the main contaminants were ^{21}Na , ^{22}Mg , and ^{16}N , in decreasing order of intensity as identified with the standard ΔE -time-of-flight method. The beam rate was about 2000 ^{23}Al ions per second. To optimize the ^{23}Al beam energy and range, a 2-mm-thick rotatable aluminum degrader, located directly in front of the detection system, was used.

A detailed description of GADGET can be found in Ref. [47]. Briefly, the assembly contains the Proton Detector, which is a cylindrical vessel filled with gas (set to 780 Torr of P10 for this experiment) that functions both as a beam stop and a charged-particle detection medium, surrounded by the Segmented Germanium Array (SeGA) [51] for coincident γ -ray detection. The beam was operated in a pulsed mode where ^{23}Al ions ($T_{1/2} = 470$ ms) were accumulated in the Proton Detector for 0.5 s, and then the beam was stopped for another 0.5 s to allow their charged particle decay radiations to be detected by ionization. The ionization electrons were drifted towards the readout plane by a uniform electric field of 125 V/cm and amplified by a Micromegas structure [52]. An electrostatic gating grid was used to protect the Micromegas from the large signals produced during the implantation periods. The active volume is a cylinder 40-cm long and 10 cm in diameter. The short range of the protons in the gas versus the near transparency to the β particles enables the detection of the weak low-energy protons and effectively eliminates an

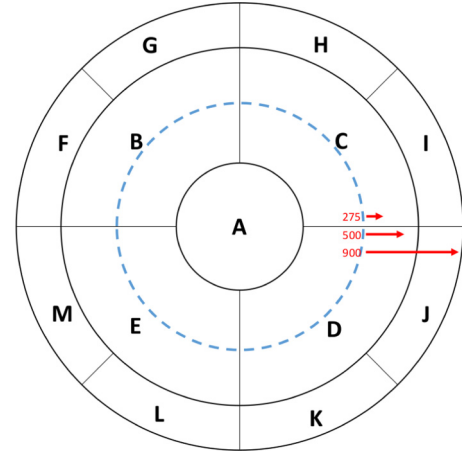


FIG. 1. Pad geometry of the anode plane of GADGET's Proton Detector. The radii of the circular borders are 1.4, 4, and 5 cm. An aperture on the cathode limits the transverse dispersion of the beam spot within ~ 2.6 cm from the center (dashed circle). Ranges of 275-, 500-, and 900-keV protons are illustrated by red arrows.

otherwise overwhelming β background. The Micromegas pad plane is divided into 13 pads, labeled A–M as shown in Fig. 1. This configuration allows vetoing of high-energy protons that might escape the active volume and deposit only part of their energy in the active volume. In addition, it enables analysis of either most of the full active volume (pads A–E) for higher efficiency or to limit the active volume into subsections to achieve lower β background at the cost of efficiency loss for higher-energy protons. In the current experiment, pads F, G, L, and M were not instrumented which resulted in 50% veto efficiency for events in the A–E active volume. However, in the case of ^{23}Al , only a small fraction of the protons are emitted above ~ 1 MeV [53], hence, the associated background is insignificant.

Figure 2 shows the proton energy spectrum for pad A (red) and for event-level summing of the five central pads (A–E, blue). The β background is substantially suppressed relative to previous experiments [45,54], allowing the extraction of

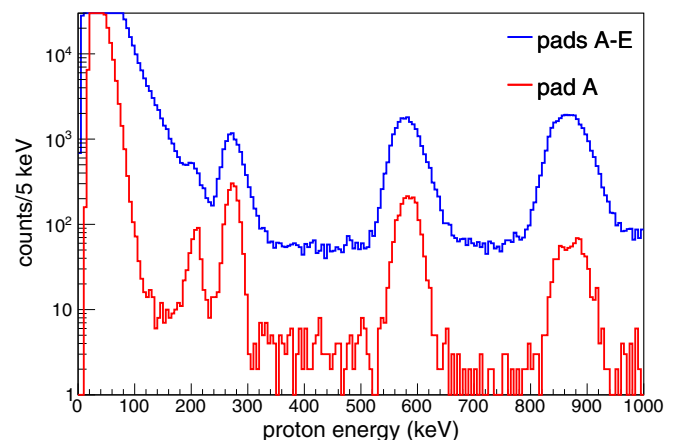


FIG. 2. Proton spectrum for pads A–E (blue) and for the central pad alone (red).

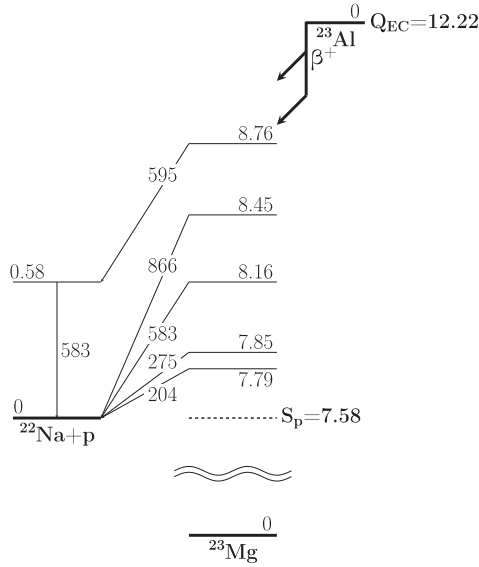


FIG. 3. A simplified decay scheme for ^{23}Al . The scheme only shows the protons with energies up to 900 keV and an associated γ ray. Level energies are given in MeV and adopted from NuDat [60], whereas proton (center-of-mass) energies are given in keV and adopted from Refs. [43,45] (except for the 595-keV protons). See the text for details.

the 204-keV peak intensity from both spectra. The single pad spectrum shows further reduced β background due to the smaller active volume, at the cost of a fast-declining efficiency as function of proton energy. There are no beam contaminants that emit β -delayed charged particles with the exception of the ^{16}N that has small α -particle branching ratio (1.2×10^{-5}). In addition, those emissions are mostly in an energy range of 1.5 to 3 MeV [55–57], which is significantly above the region of interest for this experiment. For interpretation of the proton spectrum, a simplified decay scheme is presented in Fig. 3. The energy calibration of the spectrum is internal and based on the proton peak energies reported by Ref. [43] for values up to 583 keV and in Ref. [45] for the 866-keV proton peak energy. The spectrum shows linearity with the reported proton energies. In Fig. 3, we report a transition from the 8.76-MeV state in ^{23}Mg to the first excited state of ^{22}Na , corresponding to a 595-keV proton emission. This transition is identified based on γ - p coincidences as shown in Fig. 4. The detector resolution is not sufficient to separate this proton peak from the 583-keV proton peak. However, the intensity of the coincidences is too low to account for the full intensity of the 583-keV proton peak, and the centroid of the correlated proton peak is at 595 keV. Therefore, we interpret this proton peak as a double peak with two similar energies. The corrected decay scheme should affect the interpretation of the proton intensities reported by Refs. [45,54,58,59]. We do not find the 204-keV protons in coincidence with any γ rays except for annihilation 511-keV γ rays (see Fig. 4). This confirms that the final state of the proton emission is the ground state of ^{22}Na , and, therefore, the initial state is the resonance of interest.

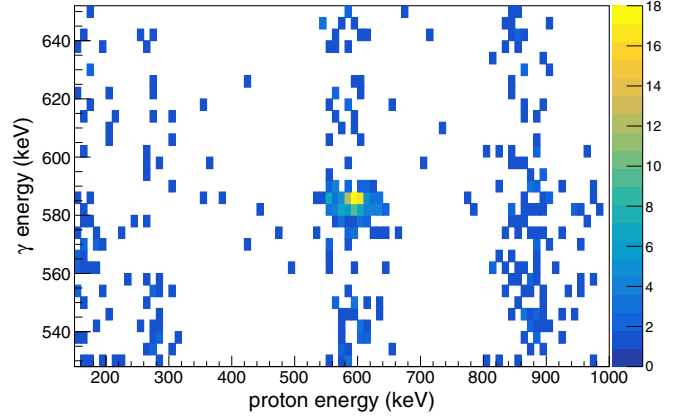


FIG. 4. Coincidence spectrum for pads A-E. No coincidence for the 204-, 275-, or 866-keV protons is seen in the spectrum, however, a coincidence between 583-keV γ rays and 595-keV protons can be seen.

The intensities of the 204-, 275-, and 583-keV peaks were normalized relative to the 866-keV peak. Although the detection efficiency of the low-energy protons is close to unity, there are some losses due to the wall effect, mostly caused by protons absorbed in the cathode and anode planes or by 866-keV protons escaping the detector's active volume. A three-dimensional GEANT4 simulation [61] was performed to calculate the efficiency corrections. For the simulation, the ^{23}Al distribution along the detector axis was extracted from the drift time of the 595-keV protons relative to the corresponding 583-keV γ rays (see Ref. [47] for details). Unfortunately, the transverse distribution of the beam is only coarsely known, based on the relative counts in the different pads, which prevents a reliable efficiency calculation of the single pad spectrum for 583-keV protons and higher. For the combined spectrum, however, the efficiency is a weak function of the transverse beam distribution due to the 5.5-cm-diameter aperture of the cathode that limits the transverse dispersion. The efficiency correction was assigned a conservative systematic uncertainty of 3% (relative) by varying the ^{23}Al distribution along both the detector axis and the transverse plane. The diffusion of the ^{23}Al atoms was calculated to be less than 1 cm within two lifetimes, hence, the effect on the transverse distribution is contained in the systematic studies. On the other hand, despite the excellent β -background suppression in the present experiment, extracting the intensity of the 204-keV peak from the combined spectrum still required modeling of the background with an exponential function, which was chosen based on the GEANT4 simulation, whereas, in the pad A spectrum, the 204-keV proton peak has a better signal-to-background ratio, and the background can be modeled with a linear function. For those reasons, we used both spectra to extract the 204-keV proton peak intensity as described below, whereas, for the other proton peaks, we used only the combined spectrum. The calculated efficiencies for the combined spectrum were $\epsilon = 0.98, 0.98, 0.97$, and 0.93 for the 204-, 275-, 583-, and 866-keV protons, respectively. Table I lists the efficiency-corrected intensities. Since the intensities of both the 583- and the 866-keV proton

TABLE I. Intensities of the low-energy ^{23}Al β -delayed proton peaks from the past [45,54,58,59] ([58] as compiled by Ref. [45]) and the present Rapid Communication, relative to the 866-keV peak intensity. Note that the 583-keV peak is contributed to by two separate decays (see the text and Fig. 3 for details).

Reference	$E_{\text{c.m.}}$ (keV)		
	204	275	583
[54]	2.2(5)	0.9(3)	0.7(1)
[58]	0.10(8)	0.13(9)	0.73(49)
[45]	0.34(6)	0.45(9)	0.69(3)
[59]	0.34(12)	0.43(15)	0.61(12)
Present Rapid Communication	0.063(4)	0.288(10)	0.685(22)

peaks were extracted precisely and accurately in a region with a good signal-to-background ratio in previous experiments, the agreement between the branching ratios of the 583-keV peak is an additional verification of the efficiency calculation. The extracted ratio for the 204-keV proton peak intensity is $I_{204}^{\beta p}/I_{866}^{\beta p} = 0.066 \pm 0.005(\text{stat.}) \pm 0.002(\text{sys.})$. An alternative approach is to use the ratio between the 204- and the 275-keV proton peak intensities in pad A alone. The short range of the 275-keV protons (see Fig. 1) relative to the active volume enables reliable extraction of this ratio. We can then use the intensity ratio between the 275-keV and the 866-keV proton peaks in the combined spectrum to extract the ratio between the 204-keV and the 866-keV peaks. This approach yields $I_{204}^{\beta p}/I_{866}^{\beta p} = 0.060 \pm 0.005(\text{stat.}) \pm 0.002(\text{sys.})$, in agreement with the previous value. Although the systematics of both values reflect the same efficiency calculation, the statistics are practically independent, and the final value is taken by averaging the above values.

We measured the ratio of intensities of the 204- and 866-keV protons in $^{23}\text{Al}(\beta p)$ ^{22}Na decay to be $I_{204}^{\beta p}/I_{866}^{\beta p} = 0.063(4)$. To put this value into context, it is instructive to review the previous literature on the lowest-energy proton peak from $^{23}\text{Al}(\beta p)$ ^{22}Na decay (Table I). As suggested by Ref. [45], it seems likely that the peak in Tighe *et al.* [54] is really a misinterpreted low-energy background or noise combined with a threshold and, therefore, we believe it is reasonable to disregard the measurement of Ref. [54]. The 204-keV peak intensity in Sun *et al.* [59] is consistent with

Ref. [45] but based on very limited statistics. The present value is consistent with the value reported by Peräjärvi *et al.* [58], which has large error bars, but the present value is a factor of 5 lower than the value in Ref. [45]. The unique systematic effect in Ref. [45] was related to the use of a Si implantation detector for which a very large subtraction of background from β particles was required to extract the proton spectrum at the lowest energies. The present Rapid Communication was carried out with a gas-filled detector specially designed to mitigate β -particle background in the region of interest, strongly reducing uncertainties associated with background subtraction. The gas-Si telescope used in Ref. [58] was also relatively insensitive to β -particle backgrounds. Therefore, we consider the present value and the one from Ref. [58] to be the most reliable. The present value provides a much smaller uncertainty that can be attributed, in part, to several orders-of-magnitude higher statistics.

Using the present value for the ratio $I_{204}^{\beta p}/I_{866}^{\beta p}$, we determine the absolute intensity of the 204-keV peak by adopting the absolute intensity of the 866-keV peak from Ref. [45], $I_{866}^{\beta p} = 0.41(1)\%$. The adopted value for the intensity of the 866-keV proton peak is relatively insensitive to systematic effects because of its higher energy and intensity, and it is also consistent with the absolute intensity of Ref. [59], albeit with large uncertainty. The result is $I_{204}^{\beta p} = 0.0257(17)\%$. Reference [46] indicated a branching ratio on the order of 0.02%, consistent with our current value. The ratio of this value to its sum with the well-known $\beta\gamma$ intensity through the same 7.79-MeV state of ^{23}Mg , $I_{7.79}^{\beta\gamma} = 3.95(37)\%$ [45,63,64] yields a proton branching ratio of $\Gamma_p/\Gamma = 6.5(8) \times 10^{-3}$.

In order to calculate the resonance strength using our new value for the proton branching ratio, we must adopt a spin and lifetime for the resonance. Multiple arguments have been made for a $(7/2)^+$ spin and parity assignment, which we adopt Refs. [45,60,65]. The only finite literature value for the lifetime is $\tau = 10(3)$ fs from an in-beam γ -ray spectroscopy measurement [41]. Using these values would lead to a resonance strength of $\omega\gamma = 0.24(8)$ meV, which is 7 and 23 times lower than the directly measured values from Refs. [34,35] and [43,44], respectively (see Table II). A recent lifetime measurement by Kirsebom *et al.* [62] did not yield a finite value but a 95% C.L. upper limit of $\tau < 12$ fs corresponding to a lower limit on the strength. Table II summarizes the resulting resonance strengths obtained using various values

TABLE II. Strength of the 204-keV (c.m.) $^{22}\text{Na}(p, \gamma)$ ^{23}Mg resonance. The strength for indirect values is calculated assuming various combinations of the branching ratios and lifetimes of the 7.79-MeV state and $(7/2)$ -spin assignment. Upper limits are calculated within a 90% C.L.

Method	Reference	$\omega\gamma$ (meV)		
Direct	[34,35]	1.8(7)		
Direct	[43,44]	$5.7^{+1.6}_{-0.9}$		
		Γ_p/Γ	$\tau = 10(3)$ fs [41]	$\tau < 12$ fs [62]
Indirect	[58]	$10(8) \times 10^{-3}$	0.4(3)	> 0
Indirect	[45]	$3.7(9) \times 10^{-2}$	$1.4^{+0.5}_{-0.4}$	> 0.71
Indirect	Present Rapid Communication	$6.5(8) \times 10^{-3}$	0.24(8)	> 0.16

for the branching ratios with both lifetimes and the direct measurement values.

The implications of adopting various resonance strengths on ^{22}Na production in novae was investigated through a series of 12 hydrodynamic simulations performed with the spherically symmetric time-implicit Lagrangian code SHIVA [66,67]. The model consists of a $1.25 M_{\odot}$ ONe white dwarf that accretes solar composition material at a rate of $2 \times 10^{-10} M_{\odot} \text{ yr}^{-1}$. Material is assumed to mix with the outer layers of the white-dwarf star as it piles up (50% solar and 50% white-dwarf material). The model was coupled to a nuclear reaction network containing 118 isotopes from ^1H to ^{48}Ti and 630 nuclear interactions. The thermonuclear $^{22}\text{Na}(p, \gamma) ^{23}\text{Mg}$ reaction rate was varied based on different assumptions about the nuclear-data inputs. The total mass of ejected material was $3.8 \times 10^{28} \text{ g}$ for all cases. The lowest output ^{22}Na mass fraction of 1.1×10^{-4} was obtained using the rates from Refs. [43,44] (consistent with the value reported in Ref. [44]). The highest output ^{22}Na mass fraction of 4.3×10^{-4} was obtained using the present branching ratio combined with the lifetime from Ref. [41] for the 204-keV resonance and the 275-keV resonance strength from Refs. [34,35]. Therefore, uncertainties associated with the $^{22}\text{Na}(p, \gamma) ^{23}\text{Mg}$ rate translate to an almost factor-of-4 variation in ^{22}Na yields from typical ONe novae corresponding to a factor-of-2 variation in maximum detectability distance for the 1.275-keV γ ray.

Using this new resonance, the strength value results in an increased ^{22}Na production and could lead to a tension between some nova nucleosynthesis models published in the literature and observational values [21,24] (on the contrary, see Ref. [68]). However, this result relies on a single lifetime measurement with 30% uncertainty. Shell-model calculations assuming spin and parity assignments of $(7/2)^+$ predict a much shorter lifetime of $\approx 0.6\text{--}1.7 \text{ fs}$ (see Ref. [69] for calculation details), yielding a resonance strength of $\omega\gamma = 1.4\text{--}4.1 \text{ meV}$, which is on the same order as the direct measurements. We,

therefore, suggest that the lifetime of the 7.79-MeV excited state of ^{23}Mg should be remeasured, ideally to a precision better than 1 fs, prior to use with the branching ratio to obtain a resonance strength. Presently, we recommend adopting the more conservative lower limit on the resonance strength based on the present branching ratio and the lifetime limit from Ref. [62].

To summarize, we have measured the low-energy ^{23}Al β -delayed proton intensities with the best accuracy so far using a new detection system GADGET [47]. The result leads to a new proton branching ratio for the key 204-keV resonance, which is a factor of 5 lower than the most precise and most recent literature value [45]. If the present value is used together with the lifetime from Ref. [41], then the resonance strength is 7 and 23 times lower than the two direct measurements Refs. [34,35] and [43,44], respectively, compounding the existing discrepancies in this resonance strength. Inconsistencies in nuclear data have now inflated the uncertainties in the ^{22}Na yield from nova models by a factor of 2. These large uncertainties suggest that the $^{22}\text{Na}(p, \gamma)$ rate is among the few important rates to constrain for modeling nova yields together with $^{18}\text{F}(p, \alpha)$, $^{25}\text{Al}(p, \gamma)$, and $^{30}\text{P}(p, \gamma)$ [67].

We gratefully acknowledge the NSCL staff for collaborating on the mechanical design and fabrication of GADGET, technical assistance, and for providing the ^{23}Al beam. We thank the NSCL γ group for assistance with SeGA. This work was supported by the U.S. National Science Foundation under Grants No. PHY-1102511, No. PHY-1565546, and No. PHY-1913554, and the U.S. Department of Energy, Office of Science, under Award No. DE-SC0016052. We also acknowledge support by the Spanish MINECO Grant No. AYA2017-86274-P by the E.U. FEDER funds and by the AGAUR/Generalitat de Catalunya Grant No. SGR-661/2017. This Rapid Communication benefited from discussions within the ChETEC' COST Action (Grant No. CA16117).

-
- [1] W. A. Mahoney, J. C. Ling, W. A. Wheaton, and A. S. Jacobson, *Astrophys. J.* **286**, 578 (1984).
 - [2] G. H. Share, R. L. Kinzer, J. D. Kurfess, D. J. Forrest, E. L. Chupp, and E. Rieger, *Astrophys. J., Lett.* **292**, L61 (1985).
 - [3] C. J. MacCallum, A. F. Hutters, P. D. Stang, and M. Leventhal, *Astrophys. J.* **317**, 877 (1987).
 - [4] R. Diehl *et al.*, *Astron. Astrophys.* **298**, 445 (1995).
 - [5] R. Diehl *et al.*, *Nature (London)* **439**, 45 (2006).
 - [6] W. Wang *et al.*, *Astron. Astrophys.* **469**, 1005 (2007).
 - [7] A. F. Iyudin *et al.*, *Astron. Astrophys.* **284**, L1 (1994).
 - [8] J. Vink, J. M. Laming, J. S. Kaastra, J. A. M. Bleeker, H. Bloemen, and U. Oberlack, *Astrophys. J. Lett.* **560**, L79 (2001).
 - [9] R. E. Rothschild and R. E. Lingenfelter, *Astrophys. J.* **582**, 257 (2003).
 - [10] M. Renaud *et al.*, *Astrophys. J. Lett.* **647**, L41 (2006).
 - [11] B. W. Grefenstette *et al.*, *Nature (London)* **506**, 339 (2014).
 - [12] S. E. Boggs *et al.*, *Science* **348**, 670 (2015).
 - [13] D. D. Clayton and F. Hoyle, *Astrophys. J.* **187**, L101 (1974).
 - [14] A. Weiss and J. W. Truran, *Astron. Astrophys.* **238**, 178 (1990).
 - [15] S. Starrfield, J. W. Truran, M. Politano, W. M. Sparks, I. Nofar, and G. Shaviv, *Phys. Rep.* **227**, 223 (1993).
 - [16] A. Coc, R. Mochkovitch, Y. Oberto, J.-P. Thibaud, and E. Vangioni-Flam, *Astron. Astrophys.* **299**, 479 (1995).
 - [17] M. Politano, S. Starrfield, J. W. Truran, A. Weiss, and W. M. Sparks, *Astrophys. J.* **448**, 807 (1995).
 - [18] J. Gómez-Gomar, M. Hernanz, J. José, and J. Isern, *Mon. Not. R. Astron. Soc.* **296**, 913 (1998).
 - [19] J. José, A. Coc, and M. Hernanz, *Astrophys. J.* **520**, 347 (1999).
 - [20] J. C. Higdon and W. A. Fowler, *Astrophys. J.* **317**, 710 (1987).
 - [21] A. F. Iyudin *et al.*, *Astron. Astrophys.* **300**, 422 (1995).
 - [22] S. Wanajo, M.-a. Hashimoto, and K. Nomoto, *Astrophys. J.* **523**, 409 (1999).
 - [23] P. Jean, M. Hernanz, J. Gómez-Gomar, and J. José, *Mon. Not. R. Astron. Soc.* **319**, 350 (2000).
 - [24] S. Starrfield, C. Iliadis, and W. R. Hix, *Publ. Astron. Soc. Pac.* **128**, 051001 (2016).
 - [25] S. Thomas *et al.*, *Astron. Astrophys.* **615**, A107 (2018).
 - [26] A. D. Angelis *et al.*, *J. High Energy Astrophys.* **19**, 1 (2018).

- [27] C. L. Fryer *et al.*, [arXiv:1902.02915](#).
- [28] S. Amari, X. Gao, L. R. Nittler, E. Zinner, J. José, M. Hernanz, and R. S. Lewis, *Astrophys. J.* **551**, 1065 (2001).
- [29] S. Amari, *New Astron. Rev.* **46**, 519 (2002).
- [30] J. José, M. Hernanz, S. Amari, K. Lodders, and E. Zinner, *Astrophys. J.* **612**, 414 (2004).
- [31] M. Bose and S. Starrfield, *Astrophys. J.* **873**, 14 (2019).
- [32] C. Iliadis, A. Champagne, J. José, S. Starrfield, and P. Tupper, *Astrophys. J., Suppl. Ser.* **142**, 105 (2002).
- [33] J. Görres, C. Rolfs, P. Schmalbrock, H. Trautvetter, and J. Keinonen, *Nucl. Phys.* **A385**, 57 (1982).
- [34] S. Seuthe *et al.*, *Nucl. Phys.* **A514**, 471 (1990).
- [35] F. Stegmüller, C. Rolfs, S. Schmidt, W. H. Schulte, H. P. Trautvetter, and R. W. Kavanagh, *Nucl. Phys.* **A601**, 168 (1996).
- [36] H. Schatz *et al.*, *Phys. Rev. Lett.* **79**, 3845 (1997).
- [37] S. Bishop *et al.*, *Phys. Rev. Lett.* **90**, 162501 (2003).
- [38] G. Savard, J. A. Clark, F. Buchinger, J. E. Crawford, S. Gulick, J. C. Hardy, A. A. Hecht, V. E. Jacob, J. K. P. Lee, A. F. Levand, B. F. Lundgren, N. D. Scielzo, K. S. Sharma, I. Tanihata, I. S. Towner, W. Trimble, J. C. Wang, Y. Wang, and Z. Zhou, *Phys. Rev. C* **70**, 042501(R) (2004).
- [39] M. Mukherjee *et al.*, *Phys. Rev. Lett.* **93**, 150801 (2004).
- [40] J. M. D'Auria *et al.*, *Phys. Rev. C* **69**, 065803 (2004).
- [41] D. G. Jenkins *et al.*, *Phys. Rev. Lett.* **92**, 031101 (2004).
- [42] A. Parikh, J. A. Caggiano, C. Deibel, J. P. Greene, R. Lewis, P. D. Parker, and C. Wrede, *Phys. Rev. C* **71**, 055804 (2005).
- [43] A. L. Sallaska *et al.*, *Phys. Rev. Lett.* **105**, 152501 (2010).
- [44] A. L. Sallaska *et al.*, *Phys. Rev. C* **83**, 034611 (2011).
- [45] A. Saastamoinen *et al.*, *Phys. Rev. C* **83**, 045808 (2011).
- [46] E. Pollacco *et al.*, *Nucl. Instrum. Methods Phys. Res., Sect. A* **723**, 102 (2013).
- [47] M. Friedman *et al.*, *Nucl. Instrum. Methods Phys. Res., Sect. A* **940**, 93 (2019).
- [48] F. Marti, P. Miller, D. Poe, M. Steiner, J. Stetson, and X. Wu, in *Cyclotrons and Their Applications 2001: Sixteenth International Conference*, edited by F. Marti, AIP Conf. Proc. No. 600 (AIP, New York, 2001), pp. 64–68.
- [49] A. Stolz, T. Baumann, T. Ginter, D. Morrissey, M. Portillo, B. Sherrill, M. Steiner, and J. Stetson, *Nucl. Instrum. Methods Phys. Res., Sect. B* **241**, 858 (2005).
- [50] D. Bazin, V. Andreev, A. Becerril, M. Doléans, P. Mantica, J. Ottarson, H. Schatz, J. Stoker, and J. Vincent, *Nucl. Instrum. Methods Phys. Res., Sect. A* **606**, 314 (2009).
- [51] W. Mueller, J. Church, T. Glasmacher, D. Gutknecht, G. Hackman, P. Hansen, Z. Hu, K. Miller, and P. Quirin, *Nucl. Instrum. Methods Phys. Res., Sect. A* **466**, 492 (2001).
- [52] I. Giomataris *et al.*, *Nucl. Instrum. Methods Phys. Res., Sect. A* **560**, 405 (2006).
- [53] O. S. Kirsebom, H. O. U. Fynbo, A. Jokinen, M. Madurga, K. Riisager, A. Saastamoinen, O. Tengblad, and J. Äystö, *Eur. Phys. J. A* **47**, 130 (2011).
- [54] R. J. Tighe, J. C. Batchelder, D. M. Moltz, T. J. Ognibene, M. W. Rowe, J. Cerny, and B. A. Brown, *Phys. Rev. C* **52**, R2298 (1995).
- [55] R. France, E. Wilds, N. Jevtic, J. McDonald, and M. Gai, *Nucl. Phys.* **A621**, 165 (1997).
- [56] X. D. Tang *et al.*, *Phys. Rev. C* **81**, 045809 (2010).
- [57] O. S. Kirsebom *et al.*, *Phys. Rev. Lett.* **121**, 142701 (2018).
- [58] K. Peräjärvi, T. Siiskonen, A. Honkanen, P. Dendooven, A. Jokinen, P. O. Lipas, M. Oinonen, H. Penttilä, and J. Äystö, *Phys. Lett. B* **492**, 1 (2000).
- [59] L. Sun *et al.*, *Nucl. Instrum. Methods Phys. Res., Sect. A* **804**, 1 (2015).
- [60] R. Firestone, *Nucl. Data Sheets* **108**, 1 (2007).
- [61] S. Agostinelli *et al.*, *Nucl. Instrum. Methods Phys. Res., Sect. A* **506**, 250 (2003).
- [62] O. S. Kirsebom *et al.*, *Phys. Rev. C* **93**, 025802 (2016).
- [63] V. E. Jacob, Y. Zhai, T. Al-Abdullah, C. Fu, J. C. Hardy, N. Nica, H. I. Park, G. Tabacaru, L. Trache, and R. E. Tribble, *Phys. Rev. C* **74**, 045810 (2006).
- [64] Y. Zhai, The structure of ^{23}Al and astrophysical consequences, Ph.D. thesis, Texas A&M University, 2007.
- [65] A. Saastamoinen *et al.*, *Phys. Rev. C* **80**, 044330 (2009).
- [66] J. José and M. Hernanz, *Astrophys. J.* **494**, 680 (1998).
- [67] J. José, *Stellar Explosions: Hydrodynamics and Nucleosynthesis* (CRC, Boca Raton, FL, 2016).
- [68] A. F. Iyudin, *Astron. Rep.* **54**, 611 (2010).
- [69] S. J. Jin *et al.*, *Phys. Rev. C* **88**, 035801 (2013).